Tissue conductivity anisotropy is insufficient to capture experimental lesion morphology in cardiac PFA modelling

A Petras[1], G Amoros Figueras[2], Z Moreno Weidmann[2], T García-Sánchez[3], D Viladés Medel[2], A Neic[4], E Vigmond[5,6], A Ivorra[3], JM Guerra[2], L Gerardo-Giorda[1,7]

[1] Johann Radon Institute for Computational and Applied Mathematics (RICAM), Austrian Academy of Sciences, Linz, Austria
[2] Hospital de la Santa Creu i Sant Pau, IR SANT PAU, Universitat Autònoma de Barcelona, CIBERCV, Barcelona, Spain
[3] Universitat Pompeu Fabra, Barcelona, Spain
[4] NumeriCor GmbH, Graz, Austria
[5] Liryc Heart Rhythm Disease Institute, Fondation Bordeaux University, Bordeaux, France
[6] CNRS, Bordeaux INP, IMB, University of Bordeaux, Bordeaux, France
[7] Johannes Kepler University, Linz, Austria

Abstract

Pulsed field ablation (PFA) is a promising treatment for cardiac arrhythmia, but the mechanisms of lesion formation in cardiac tissue remain unclear. Existing computational models typically assume isotropic media and rely on electric field thresholds, which fail to reproduce experimentally observed lesion morphology.

We extend our previous work by incorporating cardiac fiber orientation and anisotropic conductivity into a porcine open-chest geometry. Simulations with varying anisotropy ratios showed only minor effects on lesion dimensions, and results did not match experimental data.

These findings indicate that anisotropy alone is insufficient to explain lesion geometry in ventricular PFA, and additional mechanisms such as directional electroporation or thermal effects must be considered for accurate modeling.

1. Introduction

Pulsed field ablation (PFA) has emerged as a promising treatment for cardiac arrhythmias. Owing to its high efficiency and the absence of fatal complications associated with esophageal damage [1], it has already seen widespread adoption in atrial fibrillation ablation. Other types of arrhythmias are also expected to benefit from the efficacy of this technique in the near future.

Despite its clinical success, the mechanisms of lesion formation in cardiac tissue during PFA remain insufficiently understood. Computational modeling provides a valuable means to investigate these underlying processes. Most existing models, however, adopt highly simplified assumptions—treating cardiac tissue as isotropic media and relying on an electric field threshold to estimate tissue damage [2, 3]. While this approach has been reasonably effective in other tissues, it fails to capture the complex lesion morphology observed in cardiac applications, where multi-scale phenomena and tissue anisotropy play a critical role, as shown in [4].

Building upon our previous work, this study incorporates cardiac fiber orientation and anisotropic electrical conductivity into a detailed porcine open-chest geometry model. By exploring a range of anisotropic conductivity parameters, we aim to assess their impact on lesion formation and provide new insights into the biophysical mechanisms underlying PFA in cardiac tissue.

2. Methods

2.1. Geometry

An open-chest geometry of a porcine (57 kg) is considered with a 8 Fr catheter embedded on the epicardial surface of the left ventricle and a neutral patch at the back side of the simulated animal, as described in [4] and shown in Figure 1. Cardiac fibers are generated only on the two ventricles using a rule-based method described in [5], via NumeriCor's Studio software (www.numericor.at). Myocardial fiber orientation rotates transmurally for the left and right ventricles as well as their outflow tracts, as detailed in [5].
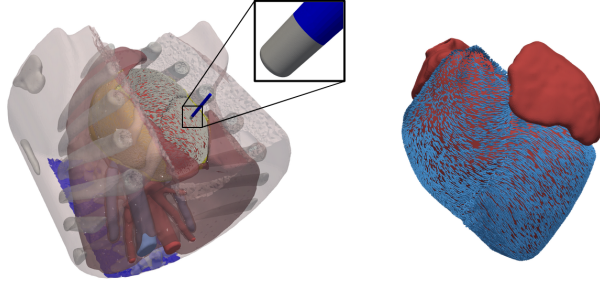
Figure 1. The open-chest geometry with the catheter embedded at the epicardial surface of the left ventricle. Cardiac fibers are considered only at the ventricles.

2.2. Mathematical model

The electric field is identified using the equation

$$\nabla \cdot (\mathbf{\Sigma}(\mathbf{E})\nabla\Phi) = 0,$$

where $\mathbf{\Sigma}(\cdot)$ is the electrical conductivity tensor that depends on the electric field $\mathbf{E} = -\nabla\Phi$ and Φ is the electrical potential. For the cardiac ventricular tissue, the electrical conductivity tensor is expressed as follows

$$\mathbf{\Sigma}(\mathbf{E}) = \sigma_f(\mathbf{E})\mathbf{f} \otimes \mathbf{f} + \sigma_t(\mathbf{E})(\mathbf{I} - \mathbf{f} \otimes \mathbf{f}),$$

where $\mathbf{f}$ are the unit vectors pointing in the fiber direction, $\mathbf{I}$ is the identity tensor and σ_f and σ_t are the electrical conductivities in the fiber and transverse directions respectively. For all other subdomains that do not feature fibers, the electrical conductivity tensor is

$$\mathbf{\Sigma} = \sigma\mathbf{I}.$$

2.3. Electroporation

The electrical conductivity of the cardiac tissue alters due to electroporation, which induces pores that disrupt the cellular membrane. Following [6], the relation of the electrical conductivity change is provided by a sigmoidal function

$$\sigma_f(\mathbf{E}) = \sigma_{f0} + \Delta\sigma\, e^{-e^{-a(\|\mathbf{E}\|-E_{thr})}},$$

$$\sigma_t(\mathbf{E}) = \sigma_{t0} + \Delta\sigma\, e^{-e^{-a(\|\mathbf{E}\|-E_{thr})}},$$

where σ_{f0} and σ_{t0} are the initial conductivities in the fiber and transverse directions, $\Delta\sigma$ is the increase in conductivity due to electroporation, a is an electrooration constant and E_{thr} is the electric field lethal threshold. We assume the same electroporation conductivity change $\Delta\sigma$, electroporation constant a and lethal threshold E_{thr} in both directions.

2.4. PFA protocol

The simulations mimic the open-chest experimental setup in [7], aiming to reproduce the experimental protocol at a burst frequency of $90\,\mathrm{kHz}$ with peak voltage of $1000\,\mathrm{V}$.

2.5. Parameters

The model parameters are summarized in the following Table 1. The electroporation related parameters are obtained from [6]. Following electrical conductivity measurements on in-vivo swines [8], the value along and across cardiac fibers is comparable at $100\,\mathrm{kHz}$. The pericardial conductivity is obtained from [9], and the values in the remaining subdomains are taken from [4].

Table 1. Summary of the model parameters.

Type	Name	Unit	Value
Torso	σ	(S/m)	0.264
Bones			10^{-2}
Lungs			0.12
Blood			1.2
Pericardium			0.17
Electrode			4.1×10^7
Thermistor			10^{-5}
Air			10^{-12}
Atria			0.44
	$\Delta\sigma$	(S/m)	0.14
	a	(m/V)	10^{-4}
	E_{thr}	(V/m)	500×10^2
Ventricles	σ_{f0}	(S/m)	0.42
	σ_{t0}	(S/m)	0.45
	$\Delta\sigma$	(S/m)	0.14
	a	(m/V)	10^{-4}
	E_{thr}	(V/m)	500×10^2

2.6. Lesion assessment

A constant lethal threshold of $500 \times 10^2\,\mathrm{V/m}$ is considered, in order to consistently assess the irreversibly damaged area for the different anisotropic electrical conductivities. The lesion dimensions measured are the lesion depth (D), width (W) and width-to-depth anisotropy ratio (W/D). Two different measurements of the width and the

anisotropy ratio are considered, one along and one across the fibers, as defined using the epicardial fiber orientation.

3. Results

The simulations were conducted using our in-house developed AblaFEMx library, which is built on the open-source FEniCSx software. An open access version of the library can be found in `https://linzlabinsilme d.github.io/`.

At first, a simulation with the average electrical conductivities from Table 1 is performed. A width-to-depth anisotropy ratio of 1.93 and 1.99 is observed along and across the fibers respectively.

Increasing the electrical conductivity ratio to (σ_{f0}/σ_{t0} = 1.2, 1.4, 1.6, 1.8 and 2 respectively, by reducing σ_{t0}, results in the lesion measurements shown in Figure 2. Note that despite increasing σ_{f0}/σ_{t0}, a minimal change in the width-to-depth anisotropy ratio occurs (its values range from 1.9 to 2 both along and across fiber orientation).
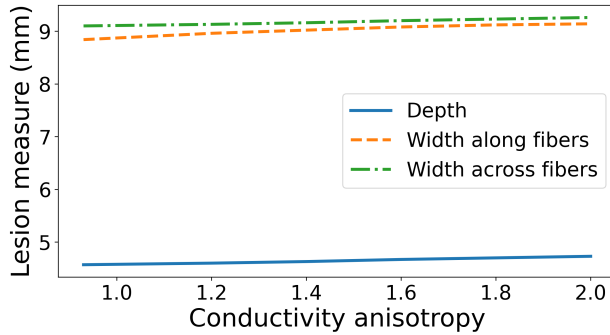

Figure 2. Lesion size measurements (depth, width along and across fibers) for the different electrical conductivity ratio (σ_{f0}/σ_{t0}) considered.

Finally, considering values that are within the experimental data in [8], in particular $\sigma_{f0} \in [0.38, 0.46]$ and $\sigma_{t0} \in [0.39, 0.54]$, Table 2 shows the results by choosing the extreme cases of $(\sigma_{f0}, \sigma_{t0}) = (0.38, 0.54)$ (with ratio 0.7) and $(\sigma_{f0}, \sigma_{t0}) = (0.46, 0.39)$ (with ratio 1.18). Regardless of the chosen values, the simulated width-to-depth anisotropy ratio is far from the experimentally observed morphology, as shown in Figure 3.

4. Discussion

This work shows that despite considering cardiac fibers in the open-chest porcine geometry, the presented model is still not rich enough to simulate lesions observed in experiments. In particular, considering both anisotropic conductivity ratio of up to 2, which nears the value reported for human tissues in [10], and porcine values measured in-vivo, the simulated lesions exhibit shapes that are far

Table 2. Lesion depth, width and width-to-depth anisotropic ratio along and across fibers of the simulated lesions using porcine anisotropic electrical conductivity parameters.

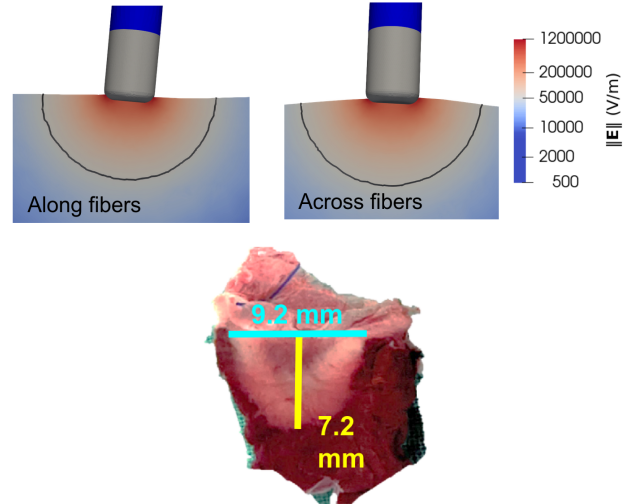| Measure $(\sigma_{f0}, \sigma_{t0})$	(0.42, 0.45)	(0.46, 0.39)	(0.38, 0.54)
D	4.57	4.55	4.59
W_{along}	8.84	8.91	8.73
W_{across}	9.1	9.07	9.14
W_{along}/D	1.93	1.96	1.9
W_{across}/D	1.99	1.99	1.99

Figure 3. Simulated lesions along and across fibers using porcine parameters (Top), do not to match the experimental lesion morphology (Bottom).

from the experimentally observed ones. This indicates that further features are required in the model, including directional electroporation damage following the fiber orientation as well as thermal effects, as suggested in [11] and [12].

5. Conclusion

Our findings indicate that the inclusion of fibers and fiber-dependent anisotropy in electrical conductivity alone is insufficient to accurately reproduce lesion geometry resulting from ventricular PFA applications.

Acknowledgments

References

[1] Gunawardene MA, Middeldorp M, Pape UF, Maasberg S, Hartmann J, Dickow J, Wahedi R, Harloff T, Matuschka S, Sultan A, Dinov B, Gessler N, Sanders P, Willems S. Esophageal endoscopic findings after pulmonary vein and posterior wall isolation using pulsed field ablation: results from the eso-pfa study. Europace 2025;27(8). ISSN 1532-2092.

[2] Gómez-Barea M, García-Sánchez T, Ivorra A. A computational comparison of radiofrequency and pulsed field ablation in terms of lesion morphology in the cardiac chamber. Scientific Reports September 2022;12(1). ISSN 2045-2322.

[3] Meckes D, Emami M, Fong I, Lau DH, Sanders P. Pulsed-field ablation: Computational modeling of electric fields for lesion depth analysis. Heart Rhythm O2 August 2022; 3(4):433–440. ISSN 2666-5018.

[4] Petras A, Amoros Figueras G, Moreno Weidmann Z, García-Sánchez T, Viladés Medel D, Ivorra A, Guerra JM, Gerardo-Giorda L. Is a single lethal electric field threshold sufficient to characterize the lesion size in computational modeling of cardiac pulsed-field ablation? Heart Rhythm O2 May 2025;6(5):671–677. ISSN 2666-5018.

[5] Doste R, Soto-Iglesias D, Bernardino G, Alcaine A, Sebastian R, Giffard-Roisin S, Sermesant M, Berruezo A, Sanchez-Quintana D, Camara O. A rule-based method to model myocardial fiber orientation in cardiac biventricular geometries with outflow tracts. International Journal for Numerical Methods in Biomedical Engineering February 2019;35(4). ISSN 2040-7947.

[6] García-Sánchez T, Amorós-Figueras G, Jorge E, Campos MC, Maor E, Guerra JM, Ivorra A. Parametric study of pulsed field ablation with biphasic waveforms in an in vivo heart model: The role of frequency. Circulation Arrhythmia and Electrophysiology October 2022;15(10). ISSN 1941-3084.

[7] Amorós-Figueras G, Casabella-Ramon S, Moreno-Weidmann Z, Ivorra A, Guerra JM, García-Sánchez T. Dynamics of high-density unipolar epicardial electrograms during pfa. Circulation Arrhythmia and Electrophysiology September 2023;16(9). ISSN 1941-3084.

[8] Tsai JZ, Will J, Hubbard-Van Stelle S, Cao H, Tungjitkusolmun S, Choy YB, Haemmerich D, Vorperian V, Webster J. In-vivo measurement of swine myocardial resistivity. IEEE Transactions on Biomedical Engineering May 2002; 49(5):472–483. ISSN 0018-9294.

[9] National Institute of Information and Communications Technology. Database of tissue dielectric properties for electromagnetic modeling of human body. `https://www2.nict.go.jp/cgi-bin/202303080003/public_html/index.py`, 2023. Accessed: 2025-09-01.

[10] IT'IS Foundation. Tissue properties database v4.2, 2024. URL `https://itis.swiss/virtual-population/tissue-properties/downloads/database-v4-2/`.

[11] Castellvi Q, Ivorra A. Computational multiscale modeling of pulsed field ablation considering conductivity and damage anisotropy reveals deep lesion morphologies. International Journal for Numerical Methods in Biomedical Engineering August 2025;41(8). ISSN 2040-7947.

[12] Miklavčič D, Verma A, Krahn PRP, Štublar J, Kos B, Escartin T, Lombergar P, Coulombe N, Terricabras M, Jarm T, Kranjc M, Barry J, Mattison L, Kirchhof N, Sigg DC, Stewart M, Wright G. Biophysics and electrophysiology of pulsed field ablation in normal and infarcted porcine cardiac ventricular tissue. Scientific Reports December 2024; 14(1). ISSN 2045-2322.

Address for correspondence:

Dr. Argyrios Petras

Johann Radon Institute for Computational and Applied Mathematics (RICAM), Austrian Academy of Sciences (ÖAW)

Altenbergerstrasse 69, 4040 Linz, Austria

argyrios.petras@ricam.oeaw.ac.at